# Carbon attachment on the aluminum nitride gate dielectric in the pentacene-based organic thin-film transistors

Hsiao-Wen Zan, Cheng-Wei Chou, Chung-Hwa Wang, Ho-Tsung Song, Jenn-Chang Hwang, and Po-Tsung Lee

Citation: Journal of Applied Physics **105**, 063718 (2009); doi: 10.1063/1.3093686
View online: http://dx.doi.org/10.1063/1.3093686
View Table of Contents: http://scitation.aip.org/content/aip/journal/jap/105/6?ver=pdfcov
Published by the AIP Publishing

# Carbon attachment on the aluminum nitride gate dielectric in the pentacene-based organic thin-film transistors

Hsiao-Wen Zan,[1,2,a)] Cheng-Wei Chou,[1] Chung-Hwa Wang,[3] Ho-Tsung Song,[2] Jenn-Chang Hwang,[3] and Po-Tsung Lee[1,2]
[1]*Department of Photonics and Institute of Electro-Optical Engineering, National Chiao Tung University, HsinChu 300, Taiwan*
[2]*Department of Photonics and Display Institute, National Chiao Tung University, HsinChu 300, Taiwan*
[3]*Department of Materials Science and Engineering, National Tsing Hua University, HsinChu 300, Taiwan*

(Received 28 October 2008; accepted 28 January 2009; published online 27 March 2009)

This study presents carbon attachment on an aluminum nitride (AlN) gate dielectric to improve the device performance of pentacene-based organic thin-film transistors (OTFTs). This approach produces high OTFT performance on an aged AlN surface. A high mobility of 0.67 $cm^2/V\,s$ was achieved on an AlN surface aged for 14 days, compared to a mobility of 0.05 $cm^2/V\,s$ on an as-deposited AlN surface. This improvement in device performance is correlated with carbon attachment on the AlN surface, which lowers surface energy. The lowered surface energy made the surface less polar, as measured by a contact angle instrument. The chemical composition of the aged AlN surface was analyzed using x-ray photoelectron spectroscopy before pentacene deposition. Enhanced C=C bonding at 284.5 eV was observed on the aged AlN surface. These enhanced C=C bonds favored the growth of large pentacene islands in the initial growth stage, which may improve OTFT device performance. © *2009 American Institute of Physics*.
[DOI: 10.1063/1.3093686]

## I. INTRODUCTION

Due to their low-temperature processing and low-cost manufacturing, organic thin-film transistors (OTFTs) are currently the focus of considerable research for applications requiring displays and flexible electronics.[1–3] However, the high operating voltage of organic transistors remains a limitation. The operating voltage can be lowered by enhancing capacitance with a thin gate dielectric[4] or a high-dielectric-constant (high-*k*) gate dielectric.[5] Aluminum nitride (AlN) is a high-*k* material with a low operating-voltage gate dielectric used in pentacene-based OTFTs.[3] AlN films have high chemical and physical stability, as well as high dielectric permittivity.[6] For pentacene-based OTFT applications, the AlN dielectric can be fabricated at a low temperature (~150 °C) using a radio-frequency (rf) sputtering system. The AlN dielectric has a similar surface energy to pentacene.[3]

This article presents a discovery of attaching carbon to the AlN gate dielectric surface that greatly improves the performance of OTFT devices. Carbon is attached on the AlN surface in a dry box before pentacene deposition. Carbon attachment is a common phenomenon that has been studied in indium tin oxide and organic light-emitting devices.[7,8] Low surface energy and high water contact angle after carbon attachment on the surface were reported.[9] In pentacene-based OTFTs, surface energy is a key issue affecting pentacene growth. Previous studies show that pentacene growth on surfaces with a low surface energy increases device performance.[10,11] Carbon attachment causes variations in surface energy, which may become an important issue in fabricating high performance OTFT devices.

## II. EXPERIMENTAL PROCEDURES

### A. Film deposition and device fabrication procedures

Heavily doped *n*-type silicon (100) wafers with a doping concentration of $5\times10^{15}$ $cm^{-3}$ were used as substrates. 1000 Å AlN film was deposited on these silicon wafers. The AlN film was deposited at a low temperature (150 °C) (substrate temperature) using a rf-sputtering system.[3,12] Before AlN film deposition, the silicon wafer was cleaned with de-ionization water (DI water) and then acetone in an ultrasonic cleaner. The wafer was then dipped in diluted HF solution ($HF:H_2O=1:100$) to remove native oxide from the silicon wafer. Finally, the wafer was immediately transferred to the rf-sputtering system. The system was set to a base pressure of less than $2\times10^{-6}$ torr before admitting gas. Mass flow controllers monitored mixed argon and nitrogen gas at an $Ar/N_2$ ratio of 2/9. The total pressure for AlN film deposition was 2.5 mtorr. All relevant experimental details have been published elsewhere.[3,12] After AlN film deposition, the samples were placed in a dry box (Ace Dragon Corporation's Dr. Storage Series, model AD315) for different periods of time, allowing the AlN surface to absorb different amounts of carbon. Humidity in the dry box was set to 35% at room temperature. A rectangular piece of pentacene (Aldrich Chemistry, not purified) defined by a shadow mask was then deposited on the AlN surface. The AlN/Si(100) substrate was heated to 70 °C during pentacene deposition at a pressure of $3\times10^{-6}$ torr. The pentacene film was 1000 Å thick, and the

a)Author to whom correspondence should be addressed. Electronic mail: hsiaowen@mail.nctu.edu.tw.

 

deposition rate was 0.5 Å/s as monitored by a quartz crystal oscillator. Finally, 100 nm thick Au pads were deposited through a shadow mask to function as the source and drain contacts. The device channel width and length were defined as 1000 and 400 $\mu$m.

### B. Characterization

X-ray photoelectron spectroscopy (XPS) (model ESCA PHI1600) was used to analyze the surface composition and chemical bonding states of a material using a monochromated Mg $K\alpha$ line at 1253.6 eV. The instrument base pressure was $5\times10^{-9}$ torr. The C 1*s* at 284.5 eV was used as a reference for all detected peak positions. To separate chemical bonding states in the XPS spectra, the spectral line shape was simulated using a suitable combination of Gaussian and Lorentzian functions.

This study used contact angle measurements to determine the migration of hydrophobic and hydrophilic functional groups. The water contact angle was sensitive to the chemical composition of the film surface.[13] The contact angles in this study were obtained by the KRŰSS contact angle system for universal surface testing (model GH-100). Material surface energy was then derived using three standard liquid contact angles (DI water, diiodo-methane, and ethylene glycol). The surface energy was calculated using Fowkes and Young's approximation, as in Eq. (1) [Eq. (1)],[14,15]

$$(1+\cos\theta)\gamma_L = 2(\gamma_S^d\gamma_L^d)^{1/2} + 2(\gamma_S^p\gamma_L^p)^{1/2}, \quad (1)$$

where $\theta$ is the measured contact angle, $\gamma_L$ is the tested liquid surface energy and is the sum of its dispersion $\gamma_L^d$ and polar part $\gamma_L^p$, and $\gamma_S^d$ and $\gamma_S^p$ are the dispersion and polar components, respectively, of solid surface free energy. The contact angles of three standard liquids (DI water, diiodo-methane, and ethylene glycol) were measured to obtain values of $\gamma_S^d$ and $\gamma_S^p$. All relevant surface energy details have been analyzed elsewhere.[16]

## III. RESULTS AND DISCUSSION

### A. Device characteristics

Pentacene-based OTFTs were fabricated on AlN dielectric surfaces that were aged in a dry box for various periods of time. Differences in aging time revealed the effect of carbon attachment on the performance of AlN dielectric OTFTs. All electrical characteristics of OTFTs were measured using Agilent 4156 and Agilent 4284 analyzers. Figure 1(a) compares the transfer characteristics of OTFTs fabricated on an as-deposited AlN surface and on an AlN surface that was aged (with carbon attached) in a dry box for 14 days. Table I lists the typical parameters of OTFTs extracted from the data in Fig. 1(a), including mobility, threshold voltage, $I_{on}/I_{off}$ current ratio, subthreshold swing, and interface state density ($N_{S.S.}$). The mobility and threshold voltage values are extracted by the slope and intercept of the square root of drain current ($I_D$) versus gate voltage ($V_G$) curves in Fig. 1(a), respectively. The interface state density was extracted using Eq. (2), as proposed in Ref. 17,

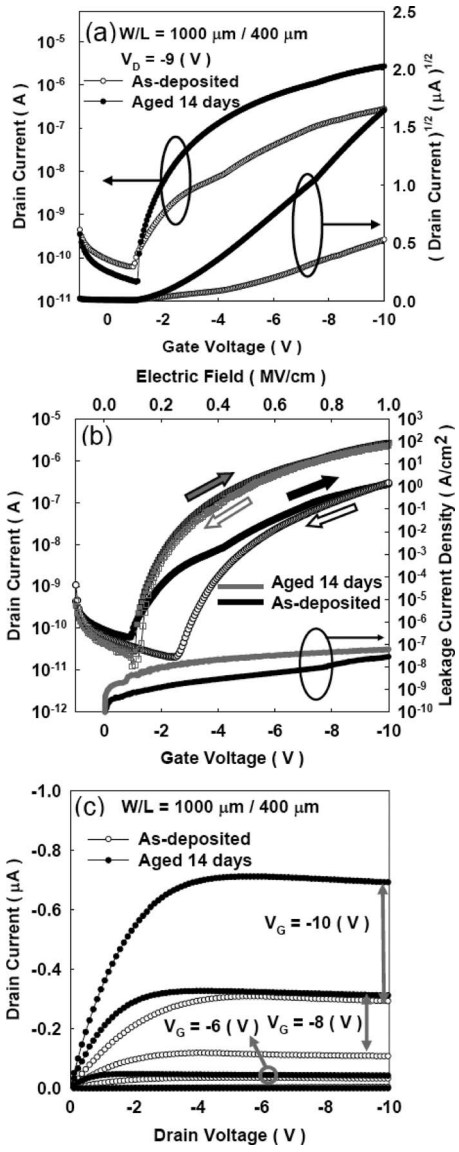


FIG. 1. (a) The transfer characteristics of OTFTs fabricated on the as-deposited AlN surface and on the AlN surface that was aged for 14 days. The square roots of $I_D$ vs $V_G$ on the respective samples plotted on the right *y*-axis. (b) The hysteresis in the transfer characteristics of OTFTs fabricated on the as-deposited and the 14 day aged AlN surfaces. The leakage-current densities of the Au–AlN–Au structures are plotted as a function of electric field for the as-deposited AlN and the 14 day aged AlN. (c) The output characteristics of OTFTs fabricated on the respective AlN surfaces.

$$N_{S.S.} = \left[\frac{S\log(e)}{kT/q} - 1\right]\frac{C_i}{q}, \quad (2)$$

where $q$ is the electron charge, $S$ is the subthreshold swing, $T$ is the temperature, $k$ is the Boltzmann constant, and $Ci$ is the insulator capacitance per unit area.

TABLE I. Extracted parameters of OTFTs under different conditions.

| | $\mu_{FE}$ ($cm^2$/V s) | $V_{TH}$ (V) | $I_{on}/I_{off}$ | S.S. (V/decade) | $N_{S.S.}$ ($cm^{-2}$ $eV^{-1}$) |
|---|---|---|---|---|---|
| As-deposited | 0.05 | −2.2 | $4.5\times10^3$ | 0.64 | $3.8\times10^{12}$ |
| Aged 14 days | 0.67 | −2.37 | $9.9\times10^4$ | 0.20 | $0.91\times10^{12}$ |

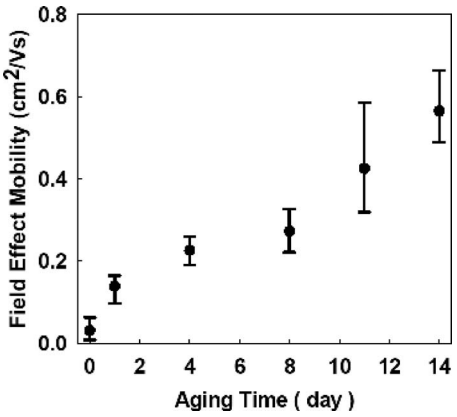


FIG. 2. Field effect mobility ($\mu_{FE}$) of OTFTs on AlN surfaces as a function of aging time.

Figure 1(b) shows the hysteresis of OTFT transfer characteristics [Fig. 1(a)]. OTFTs fabricated on the 14 day aged AlN surface markedly outperformed OTFTs on the as-deposited AlN surface. OTFTs fabricated on the 14 day aged AlN surface exhibited steep subthreshold characteristics (S.S.), low hysteresis, high field effect mobility ($\mu_{FE}$) in the saturation region, and low interface trap density ($N_{S.S.}$). The right side of Fig. 1(b) shows the leakage-current densities of the AlN dielectrics (aged or not), which were measured using the Au/AlN/Au structure. The top of this figure also shows the electric field across the Au/AlN/Au structure. The leakage-current density on the 14 day aged AlN surface slightly increases. This increase in leakage-current density indicates the existence of an additional route for charge to transfer after the exposure of AlN to air. Note that the leakage-current densities in all samples aged for 14 days are below $10^{-7}$ A/cm$^2$, which still meets OTFT requirement.

Figure 1(c) plots the output characteristics of OTFT samples. A higher output current occurs in OTFTs fabricated on the aged AlN surface. Figure 2 compares the field effect mobilities of OTFTs fabricated on AlN surfaces aged at various times. In the field of organic electronics, mobility usually varies from device to device. The level of variation is expressed by an error bar that was calculated from five different devices with the same fabrication condition. Higher field effect mobilities occur for the pentacene-based OTFTs fabricated on aged AlN surfaces. Mobility increases with the AlN surface aging time. OTFTs fabricated on the 14 day aged AlN surface exhibited the highest mobility at 0.67 cm$^2$/V s. This improved carrier transport is attributed to the pentacene growth on the carbon attached AlN surface. The following sections describe and discuss this carbon attachment phenomenon and influence for pentacene-based OTFTs.

### B. AlN film surface energy

Low dielectric surface energies can improve the carrier mobility of pentacene-based OTFTs.[10,11] Research shows that hydrophobic dielectrics provide a low energy surface that matches pentacene thin films. The hydrophobic surface (low surface energy) enables the pentacene molecules to align vertically in favor of carrier hopping among the $\pi$-orbitals, thus improving electrical characteristics.[11]

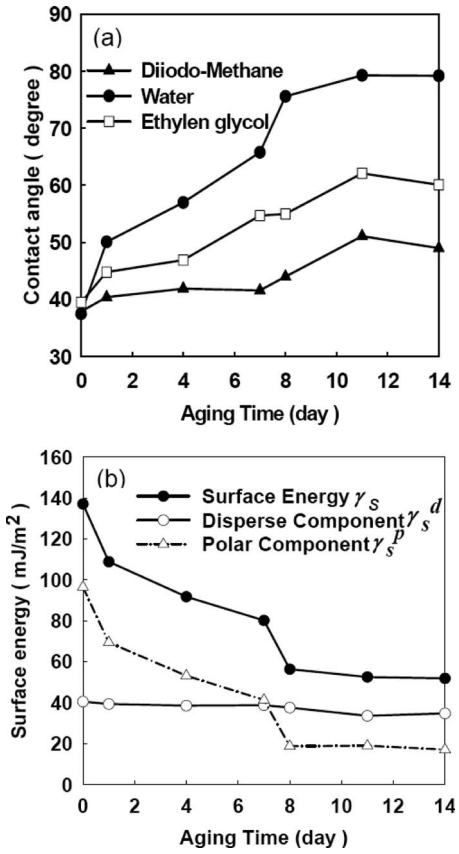


FIG. 3. (a) Water contact angles and (b) the corresponding surface energies on the AlN surface as a function of aging time.

The circle symbol in Fig. 3(a) represents the water contact angles on the AlN surface over various aging times. The water contact angles are approximately 38.3° on the as-deposited AlN surface and 79.2° on the AlN surface aged for 14 days. The water contact angle increases with aging time. The surface energy is derived from the measured liquid contact angles of DI water, diiodo-methane, and ethylene glycol in Fig. 3(a). Figure 3(b) plots the surface energy and their corresponding polar and dispersive components. The surface energy and its polar component decrease as the aging time increases. This indicates that the reduction in surface energy is primarily due to the decrease in the polar component. The reduction in the surface energy's polar component over aging time is attributed to carbon attachment based on the XPS C 1*s* spectra presented in Sec. III C.

### C. Surface chemistry of aged AlN film

To understand the surface chemistry of carbon on an aged AlN surface, the AlN surfaces were characterized using XPS. Figures 4(a) and 4(b) show the XPS C 1*s* spectra from the as-deposited and 14 day aged AlN surfaces. The curve-fit data in Figs. 4(a) and 4(b) indicate that the C 1*s* signal consists of a C=C peak at 284.5 eV, a C–O peak at 286.7 eV, and an O–C=O peak at 288.5 eV.[18–20] An increased C=C peak intensity appears on the aged AlN surface. The enhanced C 1*s* peak at 284.5 eV corresponds to C=C bonds, suggesting the occurrence of carbon attachment on AlN sur-

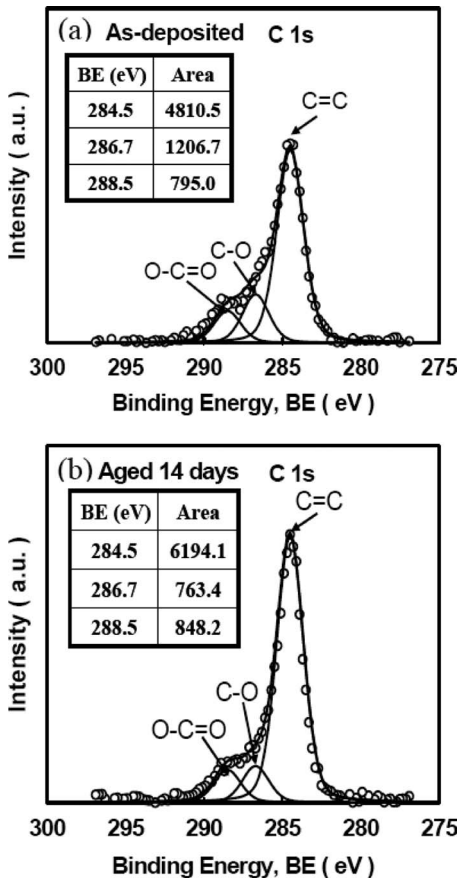


FIG. 4. XPS spectra of C 1*s* core levels from the (a) as-deposited and (b) 14 day aged AlN surface. The binding energy (BE) position and peak area of the curve-fit data are listed in the inserted table.

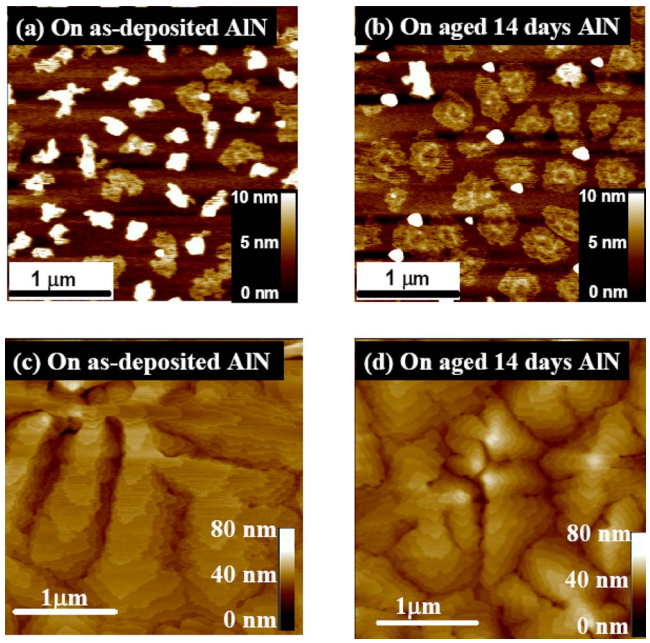


FIG. 5. (Color online) The AFM images of pentacene on (a) the as-deposited AlN and on (b) the 14 day aged AlN in the initial deposition stage. The AFM images of 1000 Å thick pentacene on (c) the as-deposited AlN surface and on (d) the 14 day aged AlN surface. The surface height is expressed by the relative contrast in the AFM images on the *z*-axis scale.

faces. The enhanced carbon attachment on the AlN surface makes the surface hydrophobic and lowers the surface energy.

The carbon required for carbon attachment to occur probably comes from the atmosphere during sample transfer or from the surface of the dry box at room temperature. However, the following argument shows that carbon in the atmosphere is most likely not the possible source of contamination. The AlN surface energy maintains the same value if the as-deposited AlN is removed from the deposited chamber and then put into a vacuum bag for 30 days at less than 1 atm using a vacuum sealing system (FoodSaver Co., model VAC550). This means that the short air exposure time before putting the AlN samples into the vacuum bag would not affect the AlN surface energy. In other words, the change in AlN surface energy is due to carbon desorption from the surface of the dry box at room temperature for a long stay time.

The signals of oxidized carbon components, C–O and O–C=O, decrease when carbon attaches to the AlN surface. This result agrees with the reduction in polar component surface energy at longer aging times in Fig. 3(b). This reduction in surface energy is thus attributed to carbon attachment that may enhance C=C bonds and reduce the relative amount of C–O and O–C=O bonds on the aged AlN surface. Carbon attachment reduces polar functional groups and surface energy to match the pentacene surface energy. Similar to the dielectric surface treated with a self-assembled monolayer (SAM) before pentacene growth, the organic SAM material increases the C=C signal on the dielectric surface and enhances the performance of pentacene-based OTFTs.[16,21,22]

### D. Pentacene morphology

The reduction in surface energy plays an important role in affecting pentacene growth and morphology. Figures 5(a)–5(d) present atomic force microscope (AFM) images of pentacene deposited on an AlN surface. These AFM images were measured using an AFM (Dimension 3100, Digital Instrument) in tapping mode. Surface roughness and surface energy affect pentacene growth. Previous research shows that surface roughness has an effect on pentacene growth.[23,24] The AlN surface roughness remains about the same after aging for 14 days. The surface roughnesses of all AlN surfaces remain at $0.24 \pm 0.02$ nm. Therefore, pentacene growth is not affected by surface roughness in this study. Figures 5(a) and 5(b) show the morphologies of pentacene islands on the as-deposited AlN surface and the 14 day aged AlN surface in the initial deposition stage. The AFM images above demonstrate that a fixed amount of pentacene deposited on the aged AlN surface creates larger islands and covers a larger area than the same amount of pentacene deposited on the as-depositing AlN surface. The fixed amount of pentacene was controlled using the same deposition rate and deposition time in the same run. Pentacene covers approximately 29% of the as-deposited AlN surface and 53% of the 14 day aged AlN surface. The larger island size and area coverage on the aged AlN surface are strongly correlated with a lower AlN surface energy due to carbon attachment. The C=C bonds on the aged AlN surface seem

to enhance the larger pentacene island growth and greater area coverage. Moreover, high pentacene coverage may produce the high OTFT performance reported by Kelley *et al.*[25] Pentacene voids seem to form more easily at the island boundaries when the pentacene islands exhibit lower coverage. The probable voids in island boundaries may limit carrier transport and decrease carrier mobility.[26] It was reported that voids and successive incomplete layers (islands) can be reduced by pentacene deposition on a low surface energy gate dielectric or a low polar energy surface.[26] These results are consistent with the surface energy, mobility, and hysteresis data presented in Secs. III A and III B.

Figures 5(c) and 5(d) show AFM images of 1000 Å thick pentacene deposited on as-deposited AlN surfaces and 14 day aged AlN surfaces, respectively. Large and dendritelike grains appear in the thick pentacene film grown on both kinds of AlN surface. The pentacene grain on the as-deposited AlN surface is larger than that on the 14 day aged AlN surface. A strong correlation exists between pentacene morphology and device performance, and a larger pentacene grain size usually exhibits higher mobility. However, the results of this study seem to show the opposite of this. The level of OTFT mobility reflects the carrier transport near the pentacene-AlN interface. The pentacene grain size at the initial stage is more dominant, as shown in Figs. 5(a) and 5(b) above. Pentacene islands are larger on the 14 day aged AlN surface than on the as-deposited AlN surface. The improved pentacene-based OTFT carrier transport on the aged AlN surface is thus attributed to larger pentacene islands near the carrier transport channel.

Moreover, the performance of OTFT devices can also be affected by various factors, including dielectric surface roughness and dielectric surface wetting properties.[23] Knipp *et al.* showed that the pentacene grain exhibits high electrical characteristics when the dielectric surface chemistry became hydrophobic. Note that the 14 day aged AlN surface is also hydrophobic, which may contribute to the higher mobility of the OTFTs.

## IV. CONCLUSION

This study investigates carbon attachment on the AlN gate dielectric in pentacene-based OTFTs and establishes the relationship between carbon attachment and electrical characteristics in pentacene-based OTFTs. The OTFTs fabricated on the AlN surface aged for 14 day exhibited greater C=C bond intensity and had a large field effect mobility. A limited aging time (14 days) enhanced the mobility of OTFTs from 0.05 to 0.67 $cm^2/V$ s. This improved mobility is due to the higher C=C bonds on the AlN surface, which lower the surface energy. This reduction in surface energy may increase the pentacene island size and area coverage in the initial stage of pentacene growth. The enhanced electrical performance of pentacene-based OTFTs is closely related to carbon attachment on the aged AlN dielectric surface. Carbon attachment should therefore be considered an important issue for developing a fabrication processes for pentacene-based OTFTs and other interface-sensitive devices.

## ACKNOWLEDGMENTS

The authors would like to thank Mr. Wei-Yu Chen at the Materials Science and Engineering Institute, NTHU for his support on ESCA measurement. This work was funded through the National Science Council of the Republic of China (Contract Nos. NSC 96-2221-E-009-127-MY2 and NSC97-2221-E-007-018-MY3) and the National Nano Device Laboratories (Contract No. P96-1A-021).

[1] S. F. Nelson, Y.-Y. Lin, D. J. Gundlach, and T. N. Jackson, Appl. Phys. Lett. **72**, 1854 (1998).
[2] C. Goldmann, S. Haas, C. Krellner, K. P. Pernstich, D. J. Gundlach, and B. Batlogg, J. Appl. Phys. **96**, 2080 (2004).
[3] H.-W. Zan, K.-H. Yen, P.-K. Liu, K.-H. Ku, and C. H. C. J. Hwang, Jpn. J. Appl. Phys. **45**, L1093 (2006).
[4] M. Halik, H. Klauk, U. Zschieschang, G. Schmid, C. Dehm, M. Schutz, S. Maisch, F. Effenberger, M. Brunnbauer, and F. Stellacci, Nature (London) **431**, 963 (2004).
[5] A.-L. Deman and J. Tardy, Org. Electron. **6**, 78 (2005).
[6] L. Valbin, L. Sevely, and S. Spirkovitch, Proc. SPIE **4174**, 154 (2000).
[7] J. A. Chaneya, S. E. Kohb, C. S. Dulcey, and P. E. Pehrsson, Appl. Surf. Sci. **218**, 258 (2003).
[8] M. G. Mason, L. S. Hung, C. W. Tang, S. T. Lee, K. W. Wong, and M. Wang, J. Appl. Phys. **86**, 1688 (1999).
[9] S. K. So, W. K. Choi, C. H. Cheng, L. M. Leung, and C. F. Kwong, Appl. Phys. A: Mater. Sci. Process. **68**, 447 (1999).
[10] C. S. Kim, S. J. Jo, S. W. Lee, W. J. Kim, H. K. Baik, S. J. Lee, D. K. Hwang, and S. Im, Semicond. Sci. Technol. **21**, 1022 (2006).
[11] W.-Y. Chou, C.-W. Kuo, H.-L. Cheng, Y.-R. Chen, F.-C. Tang, F.-Y. Yang, D.-Y. Shu, and C.-C. Liao, Appl. Phys. Lett. **89**, 112126 (2006).
[12] C.-M. Yeh, C. H. Chen, J.-Y. Gan, C. S. Kou, and J. Hwang, Thin Solid Films **483**, 6 (2005).
[13] C. M. Chan, *Polymer Surface Modification and Characterization* (Hanser Gardner, New York, 1994), Chap. 2, p. 35.
[14] D. Myers, *Surfaces, Interfaces, and Colloids: Principles and Applications*, 2nd ed. (Wiley, New York, NY, 1999), p. 430.
[15] F. M. Fowkes, J. Phys. Chem. **67**, 2538 (1963).
[16] H. W. Zan, C. W. Chou, and K. H. Yen, Thin Solid Films **516**, 2231 (2008).
[17] K. N. Narayanan Unni, S. Dabos-Seignon, and J.-M. Nunzi, J. Phys. D **38**, 1148 (2005).
[18] A. Zhu, M. Zhang, J. Wu, and J. Shen, Biomaterials **23**, 4657 (2002).
[19] G. J. Fleming, K. Adib, J. A. Rodriguez, M. A. Barteau, J. M. White, and H. Idriss, Surf. Sci. **602**, 2029 (2008).
[20] A. M. Shanmugharaj, S. Sabharwal, A. B. Majali, V. K. Tikku, and A. K. Bhowmick, J. Mater. Sci. **37**, 2781 (2002).
[21] W. Y. Chou, C. W. Kuo, Y. S. Mai, S. T. Lin, and H. L. Cheng, Proc. SPIE **5522**, 97 (2004).
[22] H. Sugimura, N. Saito, N. Maeda, I. Ikeda, Y. Ishida, K. Hayashi, L. Hong, and O. Takai, Nanotechnology **15**, s69 (2004).
[23] D. Knipp, R. A. Street, A. Vo¨lkel, and J. Ho, Appl. Phys. Lett. **93**, 347 (2003).
[24] S. E. Fritz, T. W. Kelley, and C. D. Frisbie, J. Phys. Chem. B **109**, 10574 (2005).
[25] T. W. Kelley, L. D. Boardman, T. D. Dunbar, D. V. Muyres, M. J. Pellerite, and T. P. Smith, J. Phys. Chem. B **107**, 5877 (2003).
[26] W. Y. Chou, C. W. Kuo, H. L. Cheng, Y. S. Mai, F. C. Tang, S. T. Lin, C. Y. Yeh, J. B. Horng, C. T. Chia, C. C. Liao, and D. Y. Shu, Jpn. J. Appl. Phys. **45**, 7922 (2006).